In-vivo imaging of the microvasculature of the soft tissue margins of osteonecrotic jaw lesions

P. Bastos,*[1] V. Patel,[1,2] F. Festy,[1] N. Hosny[1] and R. J. Cook[1,3]

In brief

Assesses the feasibility of RTOVI to image the soft tissue margins of exposed necrotic bone lesions in patients.

Demonstrates the feasibility of mucosal microvascular imaging in assessing the microvascular changes found in the soft tissues at the margins of osteonecrotic lesions.

Demonstrates the potential of RTOVI to inform therapeutic interventions and clinical decisions to continue or modify regime strategies in the management of patients with osteonecrosis of the jaw.

Introduction Given the increasing incidence of medication-related jaw osteonecrosis, and recognition of the mucosal blood supply's importance, we have developed a non-invasive Real Time Optical Vascular Imaging (RTOVI) instrument. Imaging the red blood cells within the sub-mucosal capillary networks demonstrates the microcirculatory anatomy. We report a small trial, demonstrating the technique's viability, examining mucosal microcirculatory changes adjacent to osteonecrotic lesions. **Aims** Imaging the microvasculature of soft tissue margins of patients' exposed necrotic bone lesions in situ was intended to provide unique observational as well as quantitative data, using an image analysis routine, based on ImageJ software. Our interest was to evaluate whether this could offer valuable information for complex wound margin management. **Methods** Four osteoradionecrosis and four medication-related osteonecrosis patients (M:F 1:1 mean 68.25 years) were enrolled under the NRES Ethics 11/LON/0354 and KCL Research Ethics Committee (REC) BDM/14/15-14 approvals. Microvascular images from mucosal margins of exposed mandibular osteonecrosis lesions were compared with equivalent images from both uninvolved contralateral mucosa and similar mucosal sites in four healthy subjects. **Results** We demonstrated narrow hypo-vascularised oedematous lesion margins surrounded by a concentric inflammatory band and normal mucosa beyond. Parameters reporting individual capillary shape, via mean percentage of occupancy per capillary per field of view and capillary loop aspect ratio, differed significantly between groups (ANOVA, $p = 0.0002$ and $p = 0.04$ respectively). Values reporting capillary number and area showed expected changes but did not reach statistical significance. **Conclusion** This pilot study demonstrated the feasibility of mucosal microvascular imaging in assessing the microvascular changes found in the soft tissues at the margins of osteonecrotic lesions, with potential to inform therapeutic interventions and clinical decisions to continue or modify regime strategies at the earliest opportunity. Given the increasing incidence of medication-related jaw osteonecrosis, and the recognition of the importance of mucosal blood supply, we developed a non-invasive instrument demonstrating microcirculation anatomy by imaging transiting red blood cells.

Introduction

Osteonecrosis of the jaw (ONJ) describes the presence of exposed necrotic bone in and around the oral cavity,[1] for which two major aetiologies are recognised: either radiotherapy- or medication-induced (bone modulating and anti-angiogenic drug therapies). Radiotherapy-induced necrosis (ORNJ), recognised for almost a century, has been joined in the last two decades by 'medication-related osteonecrosis of the jaw' (MRONJ).[2]

Despite dissimilar aetio-pathophysiologies, ORNJ and MRONJ have indistinguishable debilitating clinical presentations (Fig. 1) featuring orofacial pain, dysfunction, disfigurement, degradation of health and quality of life.[3] ORNJ is typically associated with bone hypovascularity, but the soft tissues' blood supply surrounding the exposed bone was considered normal.[4] The exact mechanisms behind ORNJ remain contentious. Meyer's trauma and superseding infection hypothesis,[5] was challenged in the 1980s by Marx, who proposed the Hypovascular/Hypocellular/Hypoxia (3H) theory, popularising hyperbaric oxygen therapies.[6] Most recently, Delanian *et al.* have suggested a 'radiation-induced fibrosis' theory, leading to contemporary pharmacological management approaches with PENTOCLO (PENtoxifylline – TOcopherol – CLOdronate).[7] No one theory has been internationally adopted and treatment of ORNJ continues to vary based on the clinician's accepted theory.

Similarly, the pathophysiology for MRONJ is also poorly understood. Theories proposed include altered bone remodelling or over suppression of bone resorption, angiogenesis inhibition, constant micro trauma, suppression of innate or acquired immunity, vitamin D deficiency, soft tissue bisphosphonate toxicity, and inflammation or infection.[2]

There appear to be no reliable curative management therapies: current approaches

[1]Dept. Tissue Engineering & Biophotonics KCL Dental Institute, Guy's Campus, London, SE1 9RT; [2]Dept. Oral Surgery GSTFT & KCL Dental Institute, Guy's Campus, London, SE1 9RT; [3]Dept. of Oral Medicine, GSTFT & KCL Dental Institute, Guy's Campus, London, SE1 9RT
*Correspondence to: Dr Pedro Bastos
Email: antonio.bastos@kcl.ac.uk

Refereed Paper. Accepted 13 September 2017
DOI: 10.1038/sj.bdj.2017.888

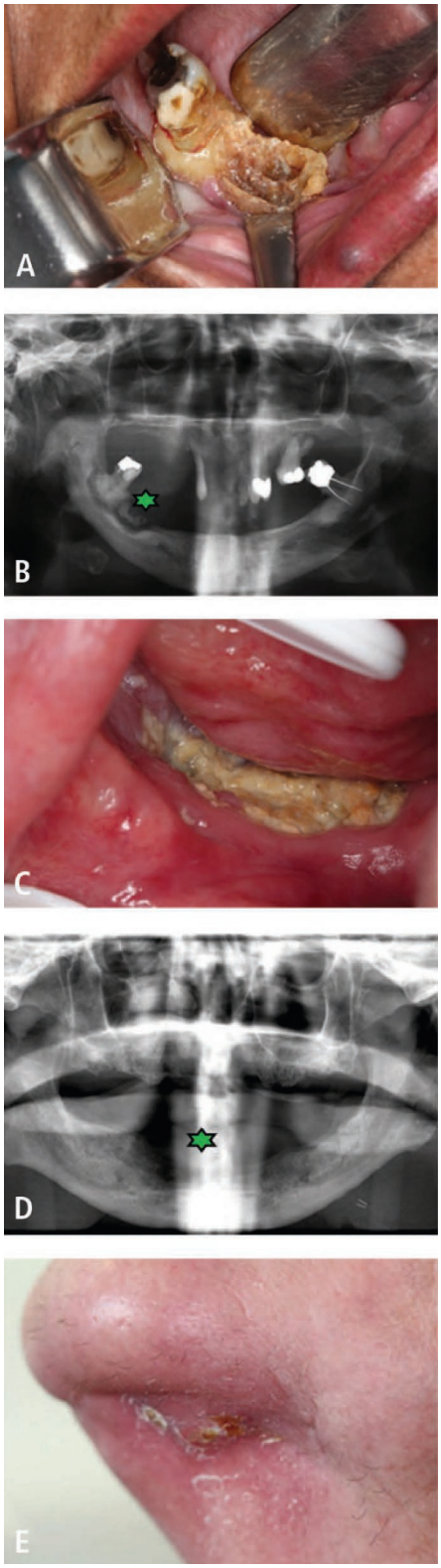

Fig. 1 Typical clinical appearances and panoramic tomograms of MRONJ (A, B), ORNJ (C, D), showing the similarities in presentation of the osteosclerotic dead bone (asterisk) in the two conditions. Should infection drain to the outer skin, significant disfiguring wounds such as an extra-oral fistula can result; that shown in figure (E) caused by ORNJ

are symptomatology-driven pharmacological strategies employing analgesics, anti-fungals, antibiotics and topical antiseptics. Surgery is only considered as a last resort, reflecting jeopardised loco-regional healing capacities.

One clear similarity is the predilection of both conditions for the mandible,[8,9] possibly reflecting lower jaw age-related blood supply degradation, the bias shifting from mandibular arterial, towards muco-periosteal supply. This is a critical observation as any influence upon the local superficial blood supply has profound influence on ORNJ and MRONJ outcomes. This mandates understanding local superficial microvasculature in monitoring and management decisions.

Formation of new blood vessels from established microcirculations (angiogenesis) is a normal part of embryonic and later tissue growth, but is also involved in pathological situations such as chronic inflammation and tumour growth.[10–12] In inflammation, some microvascular changes relate to recruitment of un-perfused circuits (cf. emotional blushing) or reduced perfusion (for example, in high tissue turgor oedematous zones or the pallor of fear).

Point-of-care microvascular assessments such as nailfold capillary pattern changes in scleroderma and Raynaud's phenomenon can reduce reliance upon invasive diagnostic procedures such as biopsy.[13–16] Sublingual microvascular flow monitoring may be used in intensive care, guiding fluid replacement in haemodynamically unstable critically ill patients.[17–19] Within the oral cavity, oral lichen planus and oral cancer microvascular changes have been reported.[10,20] However, results from these studies were primarily descriptive, offering limited quantitative data upon which to base reliable diagnostic decisions. In addition, many such studies used white light imaging, potentially hampering image quality due to poorer contrast between vessels and background tissues making some structures harder to identify.[21,22] In most previous studies, individual images are assessed by hand and latterly by some digital assessments, however automated quantification of more representative serial clinical microvascular imaging sequences, remains elusive.[23]

Benefiting from the advent of modern, fast, high-resolution detectors, and more efficient endoscopic instrumentation, we developed Real Time Optical Vascular Imaging (RTOVI). This enabled higher resolution and better contrast microscopic imaging of the micro-vasculature in real time, *in-situ* and without prior patient preparation. The instrument images red blood cells moving within the microcirculation, demonstrating the microvascular anatomy shapes and patterns.

We have already reported an initial study examining the gingival microvasculature of healthy volunteers,[24] which demonstrated RTOVI's clinical feasibility. This mandated pathological oral tissue studies, here examining previously un-reported soft tissue margin changes around osteonecrotic mandibular lesions.

Current ONJ assessment techniques are limited to macroscopic structure resolution such as regions of involved bones. Furthermore, well established vascular imaging techniques such as magnetic resonance imaging and computer tomography angiography do not offer sufficient spatial resolution and satisfactory contrast to be effective for microvascular resolution imaging.[22,25] While the necrotic bone is a primary issue, mucosal healing crucially depends on the microvascular innovation at the wound margin, yet this has been serially ignored to date.

Aims

This study aimed to assess the feasibility of RTOVI to image the soft tissue margins of exposed necrotic bone lesions in patients, to provide quantitative as well as observational data, and trial an image analytical routine based on ImageJ software. Our interest is to evaluate whether this could offer valuable guidance for complex wound margin management.

Materials and methods

Over 18 months from October 2015, four patients with well established ORNJ and four with MRONJ were prospectively consented to participate, while attending Guy's Dental Hospital Jaw Necrosis Clinic. The M:F ratio was 1:1 and mean age 68.25 years. (54-88 range). Following the American Association of Oral & Maxillofacial Surgeons[2] and Notani[26] staging respectively, only MRONJ and ORNJ stage I and II cases were accepted, the stage III trismus component possibly imposing unnecessary difficulties on volunteers. The co-morbidities associated with these patients included: types I & II diabetes, hypertension, hypercholesterolemia, anaemia, osteoporosis and

Official journal of the British Dental Association.

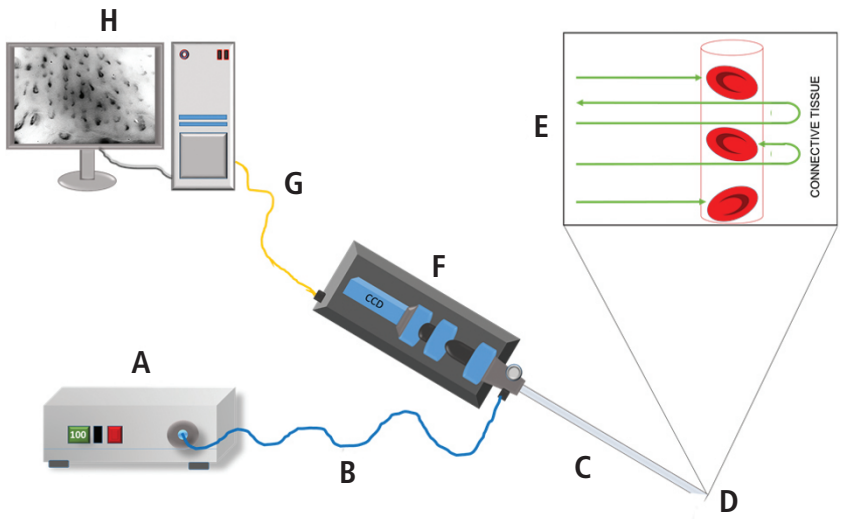

Fig. 2 Schematic light path of RTOVI system. Xenon light source (A) with a green band pass filter passing through a liquid light guide (B) into a Hopkins contact micro-endoscope (C) illuminating the tissue (D). Backscattered photons from the tissue (e) are relayed via the endoscope and coupling optics to the CCD camera connected to the PC (H) via a GigE interface (G)

hypothyroidism. In addition, same number and site microvascular anatomy images from normal oral mucosae were used for comparison (healthy control group). Both genders were equally represented in the healthy groups and the mean age was 38.4 ± 5.4 yrs. This work was approved by NRES Ethics 11/LON/0354 and KCL Research Ethics Committee (REC) BDM/14/15-14 approvals.

The soft tissues margin of exposed necrotic bone, contralateral same site intact mucosa in the same patients and same site mucosa in healthy volunteers were all imaged by a single operator utilising RTOVI.

Green (520 ± 20 nm) band-pass filtered light from a Karl Storz xenon arc source, illuminated the examined tissue via a sterile Hopkins contact colpo-hysteroscope (Fig. 2). Scattered photons from the surrounding tissues (epithelium and connective tissue) were relayed via the endoscope and dedicated optics onto a JAI CM140-GE monochrome CCD (Japan Analytical Industries) imaging at 30 frames per second with a resolution of 1392 × 1040. As red blood cells absorb green light better than surrounding tissues, high contrast images of circulating erythrocytes with a signal to noise-ratio of 4.5:1 were achieved, dynamically revealing the micro-circulation within the soft tissues (Fig. 3). 1-3 second movies were captured (30-90 frames) at 0.74 µm per pixel resolution (one red blood cell is 7-8 µm in diameter[27]), with a 1.02 mm x 0.76 mm field of view. The images were recorded using KCL in-house software (Endoscopy V17). The study movies were taken centrifugally from the bony lesion margins (Fig. 3), from the same contralateral soft tissues in each necrosis patient and from anatomically identical sites in the healthy controls.

As demonstrated in Figure 3, the images closest to the ooedematous osseous lesion

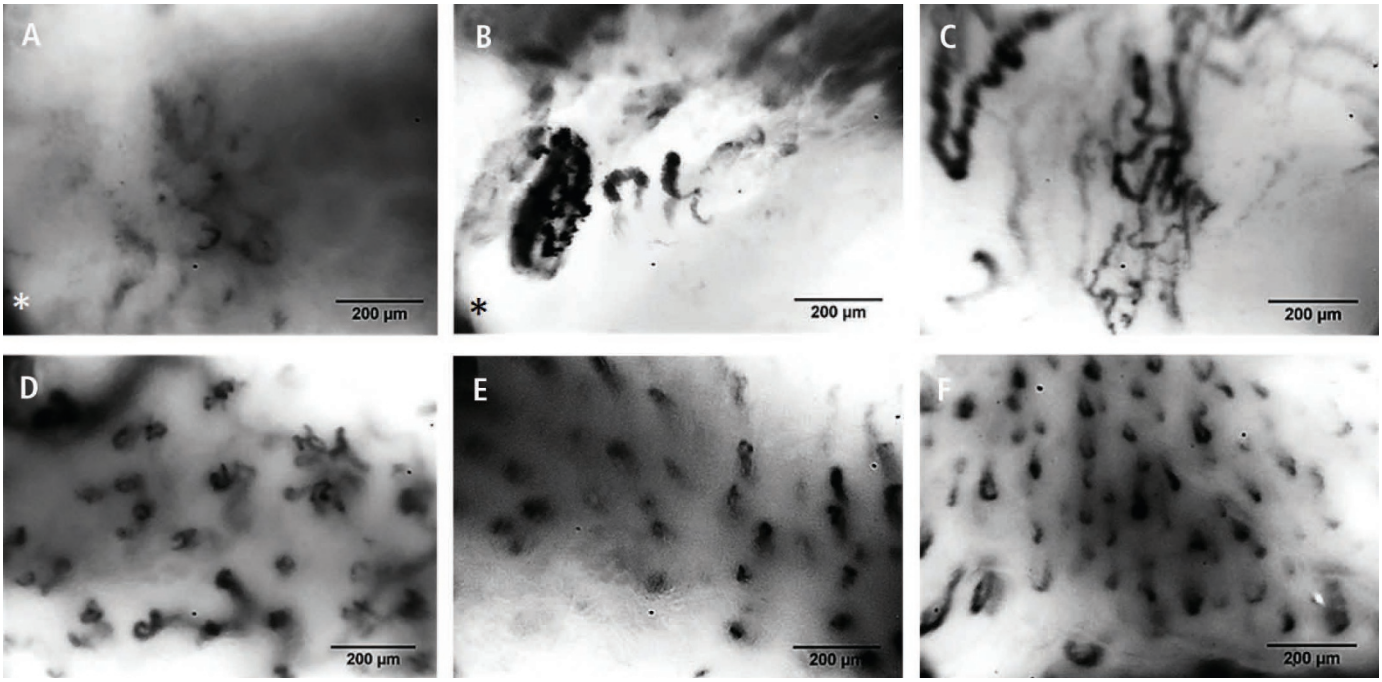

Fig. 3 Typical microvascular images, arranged as a series moving centrifugally from the osseous lesion margin (A–D). Images A & B show the oedematous gingiva immediately adjacent to an area of exposed necrotic bone. The * marks loss of tissue contact making the frame incomplete. Hypovascularity and significant capillary morphological changes are seen. Image C shows the microvasculature from the adjacent erythematous marginal gingival lesion of the same patient, demonstrating significant engorgement, aspect ratio changes and unwinding of the capillary loops than in the absolute margin tissues. D shows the microvasculature a few millimeters further out from C, demonstrating a relatively normalised micro-vascular pattern. Image E shows the relatively normal microvascular architecture of the control site of the ORNJ patient, compared with same site gingival mucosa from a healthy individual from the control group (F)

margin were markedly hypo-vascular and many were incomplete frames as the tissue rolled away from the focal plane. These were therefore not included in the assessment. The subjacent fields showed an engorged and inflamed micro-vascular pattern (Fig. 3C – intermediate zone) and were comparable to the contralateral uninvolved side and healthy volunteer control sites. Beyond this reactive rim, the vascular patterns normalised for the location.

To minimise sampling bias, the first sharp image after the mid-frame point of each sequence from each control site ORNJC (contralateral ORNJ control), MRONJC (contralateral MRONJ control) and the healthy group were compared with the same first sharp image after mid-point from the intermediate zone of ORNJ and MRONJ groups.

The entire field of view (FOV: 0.78 mm^2) from each sample image was assessed for capillary architecture. Digital analysis was performed with a series of imageJ plugins, including 'band pass filter' function, to reduce background noise, binary (black and white) format conversion and finally 'analyse particles' functions. Data yielded included the number of capillaries (density), total capillary area, area per capillary, and the mean capillary aspect-ratio (width/height of each capillary object) (MCAR) (Fig. 4). This data also allowed the mean percentage of total capillary occupancy (MPTCO) per mm^2 and mean percentage of occupancy per capillary per mm^2 (MPOPC) to be calculated. Microsoft Office 2013 Excel Anova single factor test (95% CI) was used to test the significance of differences between groups.

Table 1 Results from the quantification of microvascular data measurements from the intermediate zone from the five different sites

	MNC per mm^2	SD	MPTCO per mm^2	SD	MPOPC per mm^2	SD	MCAR	SD
ORNJ	44	16.4	9.7	3.9	0.21	0.03	2.67	0.5
ORNJC	73	11.7	10.6	1.5	0.14	0.01	2.39	0.3
MRONJ	57	36.3	11.5	6.2	0.22	0.09	3.31	0.9
MRONJC	73	15.4	7.3	2.8	0.09	0.02	2.11	0.2
HC	53	7.9	5.7	1.2	0.1	0.02	2.17	0.3

Mean number of capillaries per mm^2 (MNC), mean percentage of total capillary occupancy mm^2 (MPTCO), mean percentage of occupancy per capillary per mm^2 (MPOPC), mean capillary aspect ratio (MCAR), standard deviation (SD), osteoradionecrosis (ORNJ), osteoradionecrosis control site (ORNJC), medication related osteonecrosis of the jaw (MRONJ), medication related osteonecrosis of the jaw control site (MRONJC) and healthy control subjects (HC).

Results

The microvascular images of the soft tissue margins of exposed necrotic bone have revealed three subjective zones at the margin of osteonecrotic bone defects, irrespective of medication or radio aetiologies. Most centripetally, there is a narrow margin of tissue appearing to be hypovascular with more unwound and opened capillary features, sparsely distributed through an amorphous appearing and probably high-turgor, ooedematous tissue (Fig. 3).

This is surrounded by a region of capillary dilation and increased tortuosity, suggesting an active inflammatory response, typical of many inflammatory pathologies. Most centrifugally, more regular capillary patterns are re-established, resembling a normal healthy mucosa.

The summary quantitative measurements are shown in Table 1. The mean number of capillaries (MNC) per mm^2 was lower in both active ORNJ 44 ± 16/mm^2 and MRONJ 57 ± 36/mm^2 wound margins, compared to the contralateral control areas 73 ± 11.7/mm^2 and 73 ± 15.4/mm^2 respectively. The MNC in the healthy volunteers was 53 ± 7.9 per mm^2 (Fig. 5a). ANOVA demonstrated no significant differences between groups (p = 0.24).

The MPTCO in active wound margins was highest in patients with MRONJ, (11.5 ± 6.2%/mm^2), contrasting with, ORNJ (9.7% ± 3.9%/mm^2), MRONJC (7.3%±2.8%/mm^2), ORNJC (10.6% ± 1.5%/mm^2) and the healthy volunteers (5.7% ± 1.2%/mm^2) (Fig. 5b). ANOVA again demonstrated no significant differences between groups (p = 0.21).

The MPOPC was increased in pathology groups. ORNJ and MRONJ were, 0.21 ± 0.03%/mm^2 and 0.22% ± 0.09%/mm^2 respectively, contrasting with the control groups, ORNJC and MRONJC with 0.14 ± 0.01%/mm^2 and 0.09 ± 0.02%/mm^2 respectively, and 0.1% ± 0.02%/mm^2 in healthy volunteers

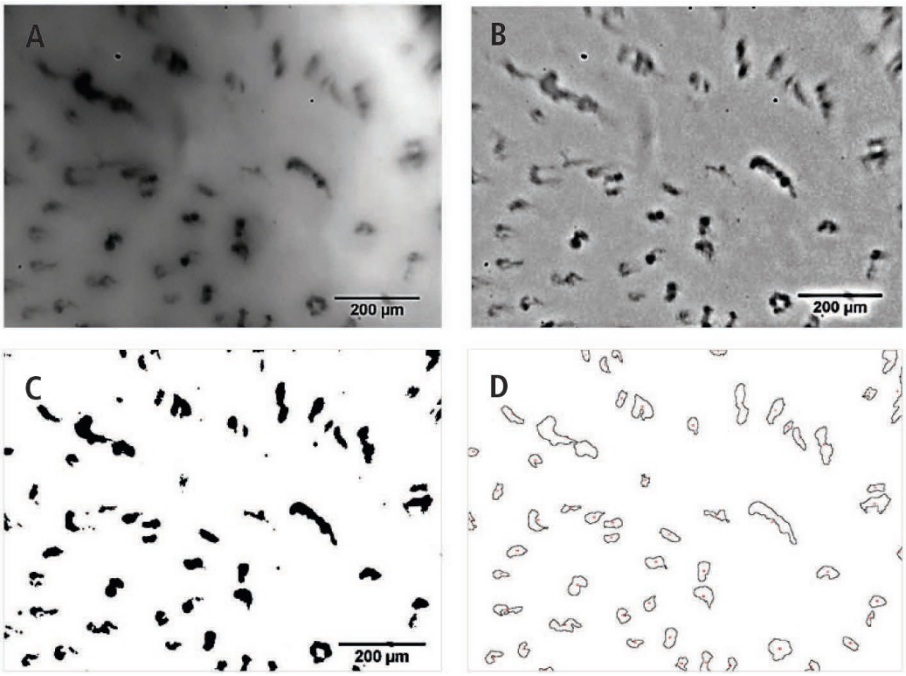

Fig. 4 Image processing and analysis using imageJ. Raw microvascular image from the gingival margin (A), image after processing with 'band pass filter' function of imageJ (B), then conversion to a binary format (C), and 'analyse particles' functions of imageJ (D), allowing digital assessment of the image

Official journal of the British Dental Association.

Fig. 5 A) Mean number of capillaries per mm² field of view. ANOVA suggested no significant differences. Data shows mean & standard deviation values. B) Mean percentage capillary occupancy per mm² field of view. ANOVA suggested no significant differences. Data shows mean & standard deviation values. C) ANOVA suggested significant differences in the Group (P = 0.0002). The Tukey- Kramer test identified ORNJ as significantly different to MRONJC and healthy controls and MRONJ as significantly different to MRONJC and healthy controls. Although not significant, the ORNJ-ORNJC relationship was similar to the MRONJ–MRONJC pattern. Data shows mean & standard deviation values. D) ANOVA suggested significant differences in the Group (P =0.04). The Tukey- Kramer test identified MRONJ-MRONJC as the only significant difference shown as the asterisked black comparison line, although ORNJ–ORNJC showed a similar relative change too. Data show mean and standard deviation values

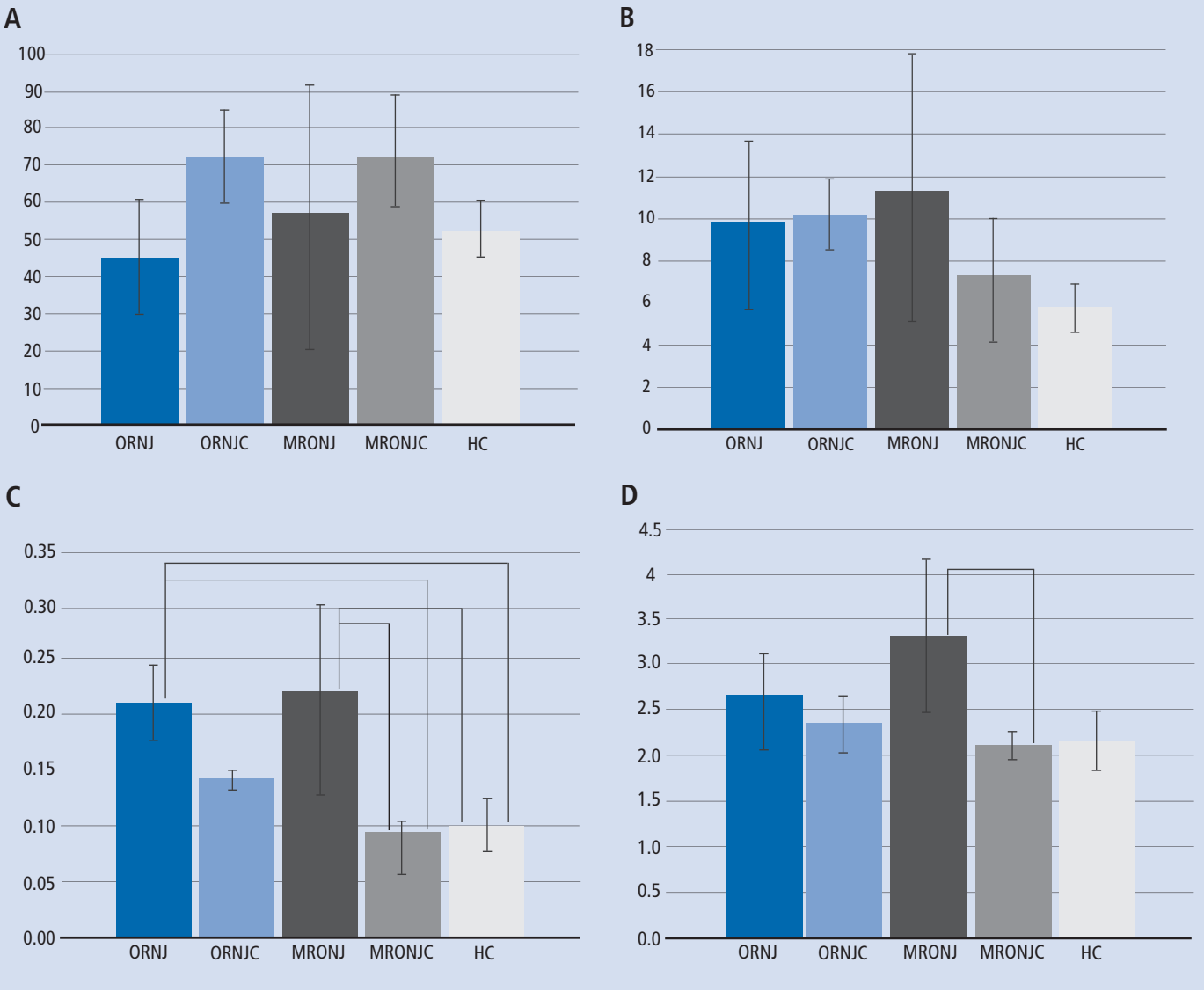

(Fig. 5c), ANOVA demonstrated significant differences between the active lesion sites and control groups (p = 0.0002).

Similarly, the MCAR was highest in active lesion ORNJ and MRONJ groups, 2.67 ± 0.5 and 3.31 ± 0.9 respectively, while the lowest value was identified in MRONJC (2.1 ±0.2) and healthy individuals (2.17 ± 0.3) (Fig. 5d). Anova highlighted a significant difference in the group (p = 0.04).

The Shapiro-Wilk test was used to confirm normal distribution of the data, permitting use of the Tukey-Kramer post-hoc test to identify the significant inter-group variations within the MPOPC and MCAR groups (Figs 5c-d).

Discussion

This small observational study showed that microvascular imaging can clearly demonstrate changes in the microcirculation alongside pathological entities and evidence tissue processes occurring subjacent to the mucosal basement membrane, in this case, associated with ORNJ and MRONJ lesions. The advantages for diagnostics and therapeutic monitoring are clear in that this is a light touch, noninvasive imaging process.

Beyond qualitative descriptive findings, we attempted to quantify changes using several descriptors. Significant inter-personal variability, seen in another study[24] may have hampered our ability to identify significant differences in MNC. However, the lowest MNC was found in the ORNJ group, which is consistent with the scarring side effect of radiotherapy on the oral mucosae.[27] MNC was higher in both the contralateral controls and

the MRONJ group (which showed the widest variation). This possibly reflects the shifts in blood supply, from mandibular arterial to muco-periosteal circulations in older individuals (cf younger healthy controls), consistent with published literature.[28]

The MPTCO was higher in the MRONJ compared to the healthy control group and with the MRONJC (contralateral side), suggesting that proximity to the necrotic bone and ulcer is the greater driving force, whereas the effects of the radiotherapy may limit that expression, again perhaps by ipsi and contralateral radiation-induced scarring. The osteonecrosis cases were greater than the healthy controls, possibly reflecting age again. Although not significant by ANOVA, these variations are consistent with current opinion.

MPOPC showed significant differences (ANOVA p = 0.0002) the Tukey Kramer test indicating that both ORNJ and MRONJ demonstrated significant differences between healthy controls and MRONJC groups. The same active-contralateral control pattern was manifest in ORNJ, although the difference did not reach significance in this case (Fig. 5c). This reflects the likely effects of the inflammatory process, engorging capillaries and unwinding the loops, tending to increase the recorded dimension in the analytical software. This finding is corroborated by previous studies in oral autoimmune inflammatory conditions[10,30] suggesting that irrespective of promoter, micro-vascular inflammatory responses are similar.

The MCAR also showed significance, reporting changes in overall capillary object outline (ANOVA p = 0.04) but only MROJ showed significant differences with its contralateral control (Fig. 5d). While not achieving significance in the Tukey Kramer test, the same general trend is also seen in the ORNJ-ORNJC pair. Similarly, variability in the the healthy controls just precluded significance with any group. Increased MCAR in lesion sites possibly reflects active inflammation processes of engorgement and capillary unwinding when engorged, thus changing the aspect ratio of the capillary in the image. In the context of the MPOPC and other less robust data, it might suggest that the effect is more driven by unwinding in the less scarred MRONJ groups and perhaps more by engorgement in the radiation groups.

In a previous pilot study involving the microvascular anatomy of healthy gingival margin tissue,[24] the aspect ratio, area per capillary and total capillary area might be the most useful parameters to measure and quantify microvascular data, as there is such a wide inter-personal variation in parameters such as total capillary number per unit area. This data suggests parameters describing the shape of individual capillary loops might be more valuable in indicating behavioural responses.

It is tempting to suggest that evidence of less engorged, unwound capillaries from the outer aspects and the loss of the hypovascular acute margin, could indicate microscopic evidence of mucosal margin healing and therefore reflect therapeutic success before clinically measurable defect diameters are detectable.

To our knowledge, this was the first time that the gingival microcirculation of patients with ORNJ and MRONJ was examined in man *and in real-time*, requiring no prior patient preparation. Conventional literature reports bony rather than soft tissue histopathological differences between ORNJ and MRONJ,[1] leaving no directly comparable published material for comparison. However, it is encouraging, that our data align with other published inflammatory disorder microvascular observations.[15,30]

There are some limitations to this study, such as health (for example, microvascular consequences of diabetes[31]), mean age of patients *versus* controls[28,29] and the exclusion of only stage III cases, therefore not treating this as an individual variable. It is prohibitive to control for all such factors in an initial trial such as this and we must accept that these may have had an effect in the findings. However, we are looking for population applicable parameters, so application to a less controlled group is more representative of real-life.

We must accept that each region was represented by a single frame from a 1-3 second (30-90 frames) movie sequence. This risks erroneous reporting as white cells, platelets and non-contiguous red cell patterns could influence imaging parameters in a single frame. It remains a computational challenge to serially analyse multiple frames and produce mean data over several heartbeats, to represent the entire patent capillary system at the observation moment. However, these data do provide an impetus to do so.

Conclusions

This pilot study demonstrated the feasibility of mucosal microvascular imaging in assessing the capillary changes found in the soft tissues at the margins of osteonecrotic lesions, with potential to inform therapeutic interventions and clinical decisions to continue or modify regime strategies at the earliest opportunity. Parameters relating to capillary morphology appear more valuable as measures of total vessel number or density are undermined by great inter-personal variability in health.

Until now, assessment of patients with ONJ has been solely based on macroscopic clinical and radiological examination findings, none of which report the condition of the microvasculature or subjacent soft tissue blood supply surrounding exposed necrotic bone. This early data suggests that parameters describing changes in individual capillary shape, rather than overall number, will be more reliable disease reporters.

With increasing incidence, particularly of medication associated ONJ, it is becoming increasingly important to develop new assessment methods based on local micro-vascular behaviour, upon which the involved bone viability in particular may depend. Larger definitive studies with statistical power are mandated to validate these results, particularly as they agree with known inflammatory and radiation-induced soft tissue effects. Improved computational software methods are also clearly needed to derive more representative datasets for each patient's lesions.

Acknowledgement

The authors wish to acknowledge the kind assistance of Mr Manoharan Andiappan in guiding and reviewing the statistical data analyses.

1. Mitsimponas K T, Moebius P, Amann K *et al.* Osteo-radio-necrosis (ORN) and bisphosphonate-related osteonecrosis of the jaws (BRONJ): The histopathological differences under the clinical similarities. *Int J Clin Exp Pathol*. 2014; **7:** 496–508.
2. Ruggiero S L, Dodson T B, Fantasia J *et al.* American Association of Oral and Maxillofacial Surgeons position paper on medication-related osteonecrosis of the jaw - 2014 update. *J Oral Maxillofac Surg* 2014; **72:** 1938–1956.
3. Fan H, Kim S M, Cho Y J, Eo M Y, Lee S K, Woo K M. New approach for the treatment of osteoradionecrosis with pentoxifylline and tocopherol. *Biomater Res* 2014; **18:** 13.
4. Stanton D C, Balasanian E. Outcome of surgical management of bisphosphonate-related osteonecrosis of the jaws: review of 33 surgical cases. *J Oral Maxillofac Surg* 2009; **67:** 943–950.
5. Meyer I. Infectious diseases of the jaws. *J Oral Surg* 1970; **28:** 17–26.
6. Marx R E. A new concept in the treatment of osteoradionecrosis. *J Oral Maxillofac Surg* 1983; **41:** 351–357.
7. Delanian S L J. The radiation-induced fibroatrophic process: therapeutic perspective via the antioxidant pathway. *Radiother Oncol* 2004; **73:** 119–131.
8. Nadella K R, Kodali R M, Guttikonda L K, Jonnalagadda A. Osteoradionecrosis of the jaws: clinico-therapeutic management: a literature review and update. *J Maxillofac Oral Surg* 2015; **14:** 891–901.
9. Kim K M, Rhee Y, Kwon Y D, Kwon T G, Lee J K, Kim D Y. Medication related osteonecrosis of the jaw: 2015

Position Statement of the Korean Society for Bone and Mineral Research and the Korean Association of Oral and Maxillofacial Surgeons. *J Bone Metab* 2015; **22:** 151–165.
10. Scardina G A, Ruggieri A, Maresi E, Messina P. Angiogenesis in oral lichen planus: an *in vivo* and immunohistological evaluation. *Arch Immunol Ther Exp (Warsz)* 2011; **59:** 457–462.
11. Wang H, Yang Z, Gu J. Therapeutic targeting of angiogenesis with a recombinant CTT peptide-endostatin mimic-kringle 5 protein. *Mol Cancer Ther* 2014; **13:** 2674–2687.
12. Murphy E A, Shields D J, Stoletov K *et al.* Disruption of angiogenesis and tumour growth with an orally active drug that stabilizes the inactive state of PDGFRbeta/B-RAF. *Proc Natl Acad Sci U S A* 2010; **107:** 299–304.
13. Cutolo M, Pizzorni C, Secchi M E, Sulli A. Capillaroscopy. *Best Pract Res Clin Rheumatol* 2008; **22:** 1093–1108.
14. Ruaro B, Smith V, Sulli A, Decuman S, Pizzorni C, Cutolo M. Methods for the morphological and functional evaluation of microvascular damage in systemic sclerosis. 2015; **30:** 1–5.
15. Hughes M, Moore T, O'Leary N *et al.* A study comparing videocapillaroscopy and dermoscopy in the assessment of nailfold capillaries in patients with systemic sclerosis-spectrum disorders. *Rheumatology (Oxford)* 2015; **54:** 1435–1442.
16. Cutolo M, Smith V. State of the art on nailfold capillaroscopy: a reliable diagnostic tool and putative biomarker in rheumatology? *Rheumatology (Oxford)* 2013; **52:** 1933–1940.
17. Hutchings S, Naumann D N, Harris T, Wendon J, Midwinter M J. Observational study of the effects of traumatic injury, haemorrhagic shock and resuscitation on the microcirculation: a protocol for the MICROSHOCK study. *BMJ Open* 2016; **6:** e010893.
18. Naumann D N, Mellis C, Smith I M *et al.* Safety and feasibility of sublingual microcirculation assessment in the emergency department for civilian and military patients with traumatic haemorrhagic shock: a prospective cohort study. *BMJ Open* 2016; **6:** e014162.
19. González R, López J, Urbano J *et al.* Evaluation of sublingual microcirculation in a paediatric intensive care unit: prospective observational study about its feasibility and utility. *BMC Pediatr* 2017; **17:** 75.
20. Takano J H, Yakushiji T, Kamiyama I *et al.* Detecting early oral cancer: narrowband imaging system observation of the oral mucosa microvasculature. *Int J Oral Maxillofac Surg* 2010; **39:** 208–213.
21. Du Le V N, Wang Q, Gould T, Ramella-Roman J C, Pfefer T J. Vascular contrast in narrow-band and white light imaging. *Appl Opt* 2014; 53; 4061–4071.
22. Singh R, Mei S C Y, Sethi S. Advanced endoscopic imaging in Barrett's oesophagus: a review on current practice. *World J Gastroenterol* 2011; **17:** 271–276.
23. Carsetti A, Pierantozzi S, Aya H *et al.* Accuracy of an automatic analysis software to detect microvascular density parameters. *Intensive Care Med Exp* 2015; **3(Suppl 1):** A415.
24. Bastos P, Cook R. Real time optical vascular imaging: a potential technique for the diagnosis of mucosal disease including early oral cancer. *Prim Dent J* 2016; **5:** 86–91.
25. McDonald D M, Choyke P L. Imaging of angiogenesis: from microscope to clinic. *Nat Med* 2003; **9:** 713–725.
26. Notani K, Yamazaki Y, Kitada H *et al.* Management of mandibular osteoradionecrosis corresponding to the severity of osteoradionecrosis and the method of radiotherapy. *Head Neck* 2003; **25:** 181–186.
27. Mizrachi A, Cotrim A P, Katabi N, Mitchell J B, Verheij M, Haimovitz-Friedman A. Radiation-Induced microvascular injury as a mechanism of salivary gland hypofunction and potential target for radioprotectors. *Radiat Res* 2016; **186:** 189–195.
28. Bradley J C. The clinical significance of age changes in the vascular supply to the mandible. *Int J Oral Surg* 1981; **10 Suppl 1:** 71–76.
29. Giuseppe Alessandro S, Antonino C, Messina P. Anatomical evaluation of oral microcirculation: capillary characteristics associated with sex or age group. *Ann Anat* 2009; **191:** 371–378.
30. Scardina G A, Messina P. Morphological characteristics of microcirculation in oral lichen planus involving the lateral border of the tongue. *J Oral Sci* 2009; **51:** 193–197.
31. Rajendran P, Rengarajan T, Thangavel J *et al.* The vascular endothelium and human diseases. *Int J Biol Sci* 2013; **9:** 1057–1069.